Provided for non-commercial research and education use.
Not for reproduction, distribution or commercial use.

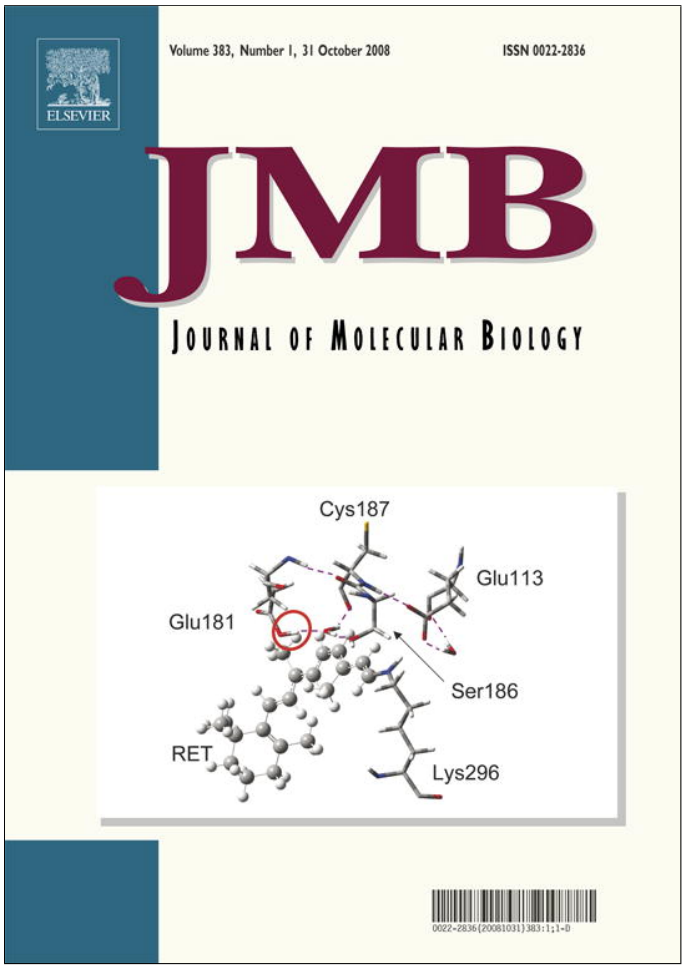

This article appeared in a journal published by Elsevier. The attached copy is furnished to the author for internal non-commercial research and education use, including for instruction at the authors institution and sharing with colleagues.

Other uses, including reproduction and distribution, or selling or licensing copies, or posting to personal, institutional or third party websites are prohibited.

In most cases authors are permitted to post their version of the article (e.g. in Word or Tex form) to their personal website or institutional repository. Authors requiring further information regarding Elsevier's archiving and manuscript policies are encouraged to visit:

http://www.elsevier.com/copyright

Author's personal copy

doi:10.1016/j.jmb.2008.08.008 J. Mol. Biol. (2008) 383, 122–132

JMB

Available online at www.sciencedirect.com

ScienceDirect

ELSEVIER

Segregation of Type I Collagen Homo- and Heterotrimers in Fibrils

Sejin Han[1,2], Daniel J. McBride[3], Wolfgang Losert[2] and Sergey Leikin[1]*

[1]*Section on Physical Biochemistry, Eunice Kennedy Shriver National Institute of Child Health and Human Development, National Institutes of Health, DHHS, Bethesda, MD 20892, USA*

[2]*Physics Department, IPST and IREAP, University of Maryland, College Park, MD 20742, USA*

[3]*Division of Endocrinology, Diabetes and Nutrition, University of Maryland School of Medicine, Baltimore, MD 21201, USA*

Received 6 June 2008; received in revised form 21 July 2008; accepted 4 August 2008
Available online 9 August 2008

Edited by M. Moody

Normal type I collagen is a heterotrimer of two α1(I) and one α2(I) chains, but various genetic and environmental factors result in synthesis of homotrimers that consist of three α1(I) chains. The homotrimers completely replace the heterotrimers only in rare recessive disorders. In the general population, they may compose just a small fraction of type I collagen. Nevertheless, they may play a significant role in pathology; for example, synthesis of 10–15% homotrimers due to a polymorphism in the α1(I) gene may contribute to osteoporosis. Homotrimer triple helices have different stability and less efficient fibrillogenesis than heterotrimers. Their fibrils have different mechanical properties. However, very little is known about their molecular interactions and fibrillogenesis in mixtures with normal heterotrimers. Here we studied the kinetics and thermodynamics of fibril formation in such mixtures by combining traditional approaches with 3D confocal imaging of fibrils, in which homo- and heterotrimers were labeled with different fluorescent colors. In a mixture, following a temperature jump from 4 to 32 °C, we observed a rapid increase in turbidity most likely caused by formation of homotrimer aggregates. The aggregates promoted nucleation of homotrimer fibrils that served as seeds for mixed and heterotrimer fibrils. The separation of colors in confocal images indicated segregation of homo- and heterotrimers at a subfibrillar level throughout the process. The fibril color patterns continued to change slowly after the fibrillogenesis appeared to be complete, due to dissociation and reassociation of the pepsin-treated homo- and heterotrimers, but this remixing did not significantly reduce the segregation even after several days. Independent homo- and heterotrimer solubility measurements in mixtures confirmed that the subfibrillar segregation was an equilibrium property of intermolecular interactions and not just a kinetic phenomenon. We argue that the subfibrillar segregation may exacerbate effects of a small fraction of α1(I) homotrimers on formation, properties, and remodeling of collagen fibers.

© 2008 Published by Elsevier Ltd.

Keywords: collagen; type I homotrimer; fibrillogenesis; segregation; osteoporosis

Introduction

Type I collagen is the most abundant structural protein found in the extracellular matrix of vertebrates. It assembles into fibrils forming the structural scaffold of bone, skin, and other connective tissues. It consists of three polypeptide α-chains folded into a 300-nm-long triple helix with short nonhelical terminal peptides (telopeptides). The triple-helical region of each chain has the distinctive amino acid repeat (Gly-X-Y) with an obligatory Gly in every third position. The amino acids in the X and Y positions vary along each chain. Frequently, X is a proline and Y is a hydroxyproline.[1]

The normal form of type I collagen is a heterotrimer of two α1(I) chains and one α2(I) chain. The chains are encoded by *COL1A1* and *COL1A2* genes located on different chromosomes. The chains have significant sequence homology, but α2(I) is more hydrophobic and has fewer proline and hydroxyproline residues. The α2(I) chain appeared in early

*Corresponding author. E-mail address: leikins@mail.nih.gov.

Abbreviations used: OI, osteogenesis imperfecta; oim, osteogenesis imperfecta murine; OD, optical density.

0022-2836/$ - see front matter © 2008 Published by Elsevier Ltd.

Author's personal copy

vertebrates and was retained through evolution in all higher vertebrates.[2,3] Nevertheless, homotrimers of three α1(I) chains form, e.g., in embryonic tissues[4] and in a variety of pathological conditions.[5–15]

Effects of α1(I) homotrimers on tissue properties are poorly understood. The evidence is conflicting. For instance, a severe bone pathology, osteogenesis imperfecta (OI), was reported in a patient whose mutant α2(I) chains were synthesized but not incorporated into collagen molecules.[11] In contrast, no such pathology was found in a few patients without any α2(I) chain synthesis.[12–14] Type I collagen in all these patients consisted entirely of α1(I) homotrimers, but the resulting disease phenotype was dramatically different.

Several studies on α1(I) homotrimer properties and interactions have been reported. It has been established that homotrimer triple helices have higher overall stability[16,17] and an altered pattern of local stability.[17] Homotrimer helices exhibit less efficient mutual recognition and weaker intermolecular attraction.[17,18] As a result, fibrillogenesis requires a higher concentration of homotrimers.[19] Homotrimer fibrils are morphologically similar to heterotrimer fibrils,[19,20] but they have lower tensile strength[21] and sparser and less precise packing of the helices.[20]

Most of the knowledge accumulated so far pertains to fibrils containing only heterotrimers or only homotrimers, although just a handful of recessive cases with no synthesis or incorporation of α2(I) chains into collagen have been reported. Much less is known about interactions of α1(I) homotrimers with the heterotrimers in mixed fibrils, formation of which may be quite common. The homotrimers were found, e.g., in cultures of some kidney[7,10] and cancer cells.[5,22–24] Moreover, cultured osteoblasts with a recently discovered *COL1A1* polymorphism were found to secrete up to 10–15% of α1(I) homotrimers.[25] Multiple studies linked this *COL1A1* polymorphism to increased bone fragility in age-related osteoporosis in the general population, sparking a renewed interest in α1(I) homotrimers.[25–28] However, it is still not clear whether and how a small fraction of the homotrimers can affect bone and whether the synthesis of the homotrimers is responsible for bone fragility.

To understand how the presence of a fraction of homotrimers may affect formation and properties of fibrils, we investigated different mixtures of heterotrimeric type I collagen from wild-type mouse tail tendon and homotrimeric collagen from homozygous osteogenesis imperfecta murine (oim) mouse tail tendon. The latter mice make a nonfunctional α2(I) chain that is not incorporated into collagen, similar to the patient with OI discussed above.[29] We measured the *in vitro* fibrillogenesis kinetics after a temperature jump from 4 to 32 °C and the equilibrium solubility of the homo- and heterotrimers at 32 °C as a function of the mixture composition. We used confocal microscopy to examine the morphology of the resulting fibrils and partitioning of homo- and heterotrimers labeled by different fluorescent dyes.

To achieve equilibration of fibrils with the surrounding solution, we pretreated the homo- and heterotrimers with pepsin at 4 °C. By partially degrading the telopeptides, pepsin prevents irreversible covalent cross-linking between the molecules.[30,31] While such a treatment alters the fibrillogenesis kinetics,[30,32] it does not affect the integrity of the triple helices and does not alter their packing and interactions in fibrils.[33]

We found that homotrimers affected the fibril bending rigidity and nucleation mechanism. More importantly, we observed equilibrium segregation of homo- and heterotrimers at a subfibrillar level. We argue that this segregation may dramatically exacerbate effects of even a small fraction of the homotrimers on tissues.

Results

Fibrillogenesis kinetics

After a temperature jump from 4 to 32°C, the turbidity of pepsin-treated heterotrimer solutions in 0.13 M NaCl, 30 mM sodium phosphate, pH 7.4, followed the expected[34] time course with lag, growth, and plateau phases (Fig. 1a, dashed line). The turbidity, which is caused by light scattering from forming collagen fibrils, was monitored by measurement of the optical density at 350 nm (OD_{350}).

In contrast, we observed no lag phase for natural homotrimers purified from oim mouse tail tendons and reconstituted homotrimers refolded from rat tail and bovine Achilles tendon collagen (Fig. 1b), consistent with a previous report.[18] Slightly different concentrations of sodium phosphate and collagen were used for collagen from different species to optimize the fibrillogenesis rate and OD_{350}.

In mixtures of heterotrimers and homotrimers, we observed four fibrillogenesis steps: 1, early growth; 2, lag phase; 3, delayed growth; and 4, plateau (Fig. 1c). The early growth was probably associated with formation of homotrimer nuclei and fibrils, while mixed and/or heterotrimer fibrils presumably formed primarily during the lag phase and delayed growth. Table 1 shows turbidity parameters extracted from the experiments in which constant, 0.3 mg/ml total concentration of collagen and various molar fractions of homotrimers were used. The final turbidity at the plateau gradually decreased with increasing homotrimer fraction, but the lag time, maximum growth rate delay, and half-maximum turbidity time appeared to change only between 0% and 50% homotrimer concentrations. Note that the plateau turbidity value may be difficult to interpret, since it depends on the number and the size of the fibrils.

Fiber morphology and molecular segregation

To test whether homo- and heterotrimers co-assembled into the same fibrils, we prelabeled them with Alexa Fluor 488 (green, G) and Alexa

Author's personal copy

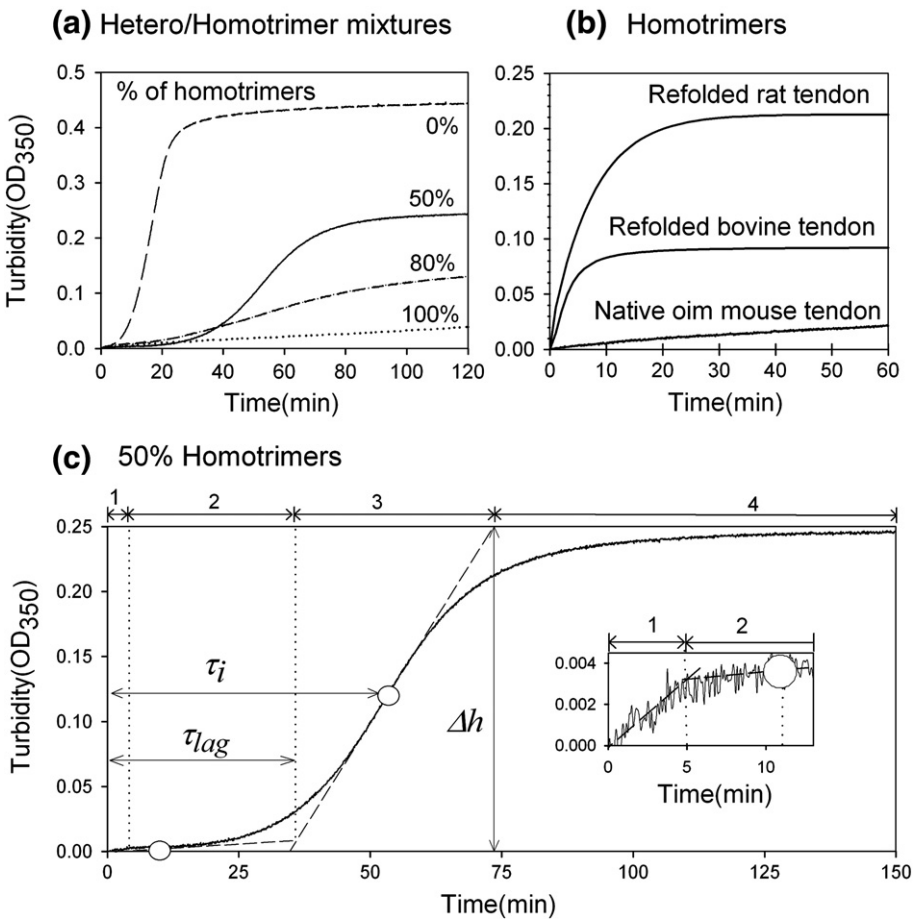

Fig. 1. Fibrillogenesis kinetics in hetero/homotrimer mixtures of type I collagen: (a) 0.3-mg/ml mixtures of type I collagen from wild-type (heterotrimers) and homozygous oim (homotrimers) mice in 30 mM sodium phosphate, 0.13 M NaCl, pH 7.4; (b) homotrimers from homozygous oim mouse tendons [100% curve in (a)], bovine Achilles tendons (refolded, 0.36 mg/ml, 30 mM sodium phosphate), and rat tail tendons (refolded, 0.25 mg/ml, 20 mM sodium phosphate); (c) 1:1 mixture of mouse heterotrimers and homotrimers [50% curve in (a)]. In (c), the white circles show two inflection points on the turbidity curve; the dashed tangential lines indicate turbidity trends at different fibrillogenesis steps; the vertical dotted lines separate four fibrillogenesis steps: 1, early growth; 2, lag phase; 3, delayed growth; and 4, high plateau; the inset shows the early kinetics. The small, lagless turbidity rise during the early growth was reproducible. It occurred only at sufficiently high homotrimer concentrations and was consistent with the rapid appearance of small aggregates observed by confocal microscopy. Note that the lag phase and high plateau might be difficult to see in (a) for the 80% curve, but both steps were clearly distinguishable when this curve was plotted separately on a larger scale.

Fluor 568 (red, R). At less than one Alexa Fluor dye per four to five collagen triple helices, we observed normal turbidity curves, critical fibrillogenesis concentrations, and fibril morphology (see below). In contrast, Cy dyes altered the fibrillogenesis kinetics curve and induced formation of nonfibrillar aggregates even at low labeling fractions.

We prepared 0.3 mg/ml hetero-G/hetero-R, homo-G/homo-R, and hetero-G/homo-R binary mixtures in 0.13 M NaCl and 30 mM sodium phosphate and equilibrated them in sealed microscopy cells at 32 °C for several hours. Here, homo- and hetero- indicate homotrimers and heterotrimers, respectively, while G and R indicate the labeling color. Subsequent examination by confocal microscopy in a controlled environment chamber set at 32 °C revealed three-dimensional (3D) networks of flexible, long heterotrimer fibrils (Fig. 2a). The homotrimers formed fewer fibrils, which looked like straight spears emanating in several directions from a clumplike common center (Fig. 2b). In homo/heterotrimer mixtures, we observed an

Table 1. Kinetic parameters of fibrillogenesis

Homotrimers (%)	Lag time (τ_{lag}, min)	Maximal growth rate delay (τ_i, min)	Half-maximal turbidity time ($\tau_{1/2}$, min)	Final turbidity (Δh)
0	9	17	16	0.46
50	36	52	54	0.25
80	26	53	55	0.13
90	34	52	74	0.09
100			55	0.04

All parameters were determined from turbidity curves as shown in Fig. 1c: τ_{lag} is the time at the end of the lag phase, τ_i is the time at the inflection point during the delayed growth step, $\tau_{1/2}$ is the time at 50% of maximal turbidity (not shown in Fig. 1), Δh is the maximal turbidity reached on the high plateau (measured at 150 min).

Author's personal copy

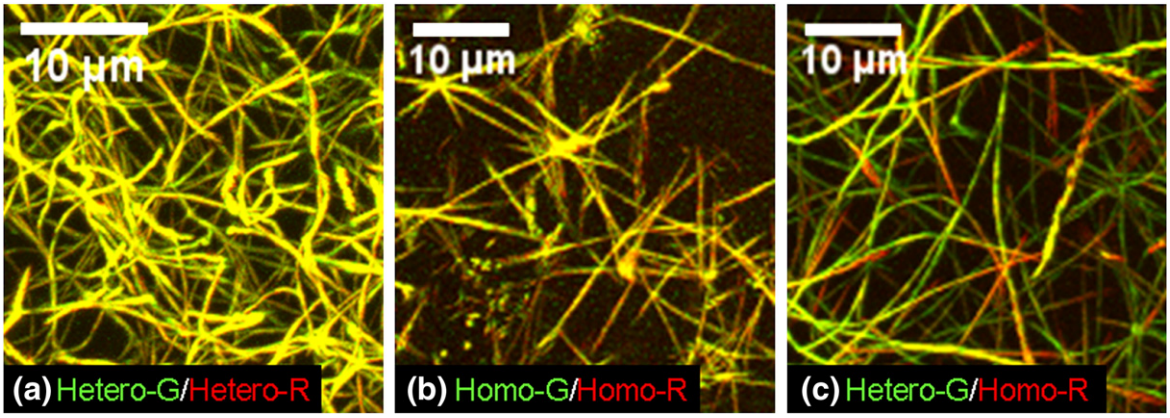

Fig. 2. 3D reconstruction of confocal images of collagen fibril networks in different 0.3-mg/ml mixtures of fluorescently labeled wild-type heterotrimers (Hetero) and oim homotrimers (Homo) from mouse tail tendons. Molecules labeled by Alexa Fluor 488 (G) are shown in green. Molecules labeled by Alexa Fluor 568 (R) are shown in red. The yellow overlay color appears in fibrils containing approximately the same amount of molecules labeled by each dye.

intermediate morphology (Fig. 2c). In particular, the fibrils appeared to be more flexible than in pure homotrimers and less flexible than in pure heterotrimers. We observed similar morphologies of unlabeled collagen fibrils by light reflection confocal microscopy.

Overlaying the green and red channels (normalized to the same total intensity within each 3D stack as described in Materials and Methods) revealed relatively homogeneous yellow fibril color in pure homotrimers and in pure heterotrimers. As expected, the G- and R-labeled molecules were evenly distributed within the fibrils. In mixtures, both heterotrimers and homotrimers appeared to be present within each fibril, but the color distribution was highly heterogeneous, particularly in thinner fibrils and at fibril tips. The G- and R-labeled molecules were unevenly distributed, forming homo- and heterotrimer-rich regions. The optical resolution was insufficient for determining whether this segregation of the homo- and heterotrimers was caused by formation of separate homo- and heterotrimer-rich microfibrils. Nevertheless, to emphasize the presence of several homo- and heterotrimer-rich regions within most fibrils, hereinafter we refer to this observation as subfibrillar segregation.

We quantified the segregation by calculating the relative excess of red color in each pixel ($I_R - I_G / I_R + I_G$) in the range −1.0 (completely green) to 1.0 (completely red). Here I_R and I_G represent the normalized red and green intensities. The resulting color separation fraction is shown by relative frequency histograms in Fig 3. In controls where the same kind of collagen was labeled with both colors (hetero-G/hetero-R and homo-G/homo-R mixtures) we observed a single peak at $I_R - I_G / I_R + I_G = 0$. In hetero-G/homo-R mixtures, however, we found two distinct peaks representing the homo- and heterotrimer-rich regions.

Note that the broadening of the homo-G/homo-R mixture histogram compared to the histogram for hetero-G/hetero-R may be caused by thinner homotrimer fibrils. For thinner fibrils, statistical variation in the number N of molecules labeled by

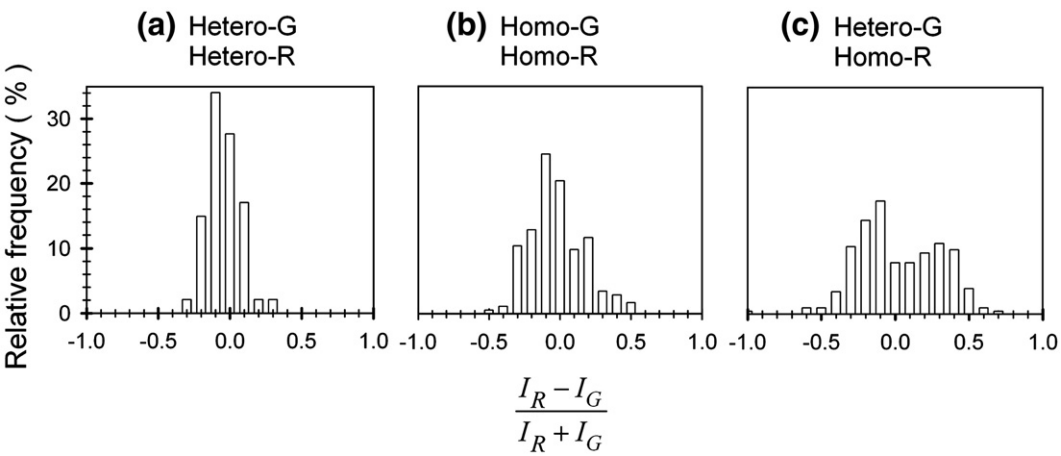

Fig. 3. Collagen segregation in mixed fibrils. Each histogram of $I_R - I_G / I_R + I_G$ fluorescence intensity ratio shows distribution of R- and G-labeled molecules.

Author's personal copy

each color within the focal volume may cause an appreciable peak broadening. In a confocal microscope, the fluorescence is collected from a small focal volume (<1 μm^3), which may contain $N \sim 1000$ or fewer labeled molecules. A smaller number of molecules in thinner fibrils will result in a larger statistical variation in $I_R - I_G / I_R + I_G$ (which is proportional to $1/\sqrt{N}$). Chromatic aberrations, producing displacement of one color with respect to the other in the image, may cause further broadening of the peak in the histogram. The same chromatic aberration will cause a larger change in $I_R - I_G / I_R + I_G$ for thinner fibrils.

Co-assembly accompanied by subfibrillar segregation also occurred when a homotrimer solution was added to preformed heterotrimer fibers. A 0.3-mg/ml solution of G-labeled heterotrimers in 30 mM sodium phosphate and 0.13 M NaCl was equilibrated for 2 h at 32 °C. Subsequent examination by confocal microscopy revealed a well-formed fibril network (Fig. 4a). A cold (4 °C) 0.3-mg/ml solution of R-labeled homotrimers in the same buffer was then injected into the heterotrimer fibril network by a micropipette to achieve ~1:3 homotrimer: heterotrimer ratio in the final mixture. Following the injection, the sample was reequilibrated at 32 °C and repeatedly reexamined by confocal microscopy in several different areas. After ~1 h, homotrimers were observed predominantly at the tips of preformed heterotrimer fibrils, creating an appearance of longitudinal fibril growth (Fig. 4b). After ~2 h, more homotrimers were observed in other fibril areas (Fig. 4c). Their distribution was more reminiscent of that observed after fibrillogenesis of premixed samples (Fig. 2c). No independent homotrimer fibrils were observed, suggesting that the interaction between a homotrimer and a heterotrimer was more favorable than between homotrimers. In contrast, injection of a cold solution of G-labeled heterotrimers to preformed R-labeled homotrimer fibrils resulted in independent formation of separate heterotrimer fibrils in addition to heterotrimer binding to preexisting fibrils (not shown).

Collagen solubility

To further investigate the segregation of homo- and heterotrimers, we systematically examined their solubility in equilibrium with mixed fibrils (sometimes referred to as a critical fibrillogenesis concentration). Different mixtures of homo- with heterotrimers in 30 mM sodium phosphate and 0.13 M NaCl, pH 7.4 (0.3–1.6 mg/ml total collagen concentration) were equilibrated for 1 day at 32 °C. Fibrillar and soluble collagens were then separated by centrifugation and fluorescently labeled with Cy5. The composition of the fibrils (pellet) and the solubilities of the heterotrimers and homotrimers (their concentrations in the supernatant) were analyzed by gel electrophoresis, relying on linear dependence of the fluorescent intensities of the gel bands on the concentration of the corresponding chains in the sample (Fig. 5a).

The first lane of the gel in Fig. 5a shows electrophoretic bands of the α1(I) chain, α2(I) chain, and covalent dimers of α1α1 and α1α2 (sometimes referred to as β11 and β12 dimers, respectively) in a 100% heterotrimer sample. The relative intensities of the α2 and α1α2 bands decreased with increasing homotrimer fraction in the sample. Only α1 and α1α1 bands were present in a 100% homotrimer sample (last lane in Fig. 5a). Based on the calibration curves for the α1/α2 and on α1α1/α1α2 intensity ratios shown in Fig 5b, we determined the homotrimer fraction in each pellet and supernatant. By comparing the intensities of the α1 bands with those of standards labeled at the same time and in identical conditions, we measured the concentration of the α1 chains in each supernatant, from which we determined the solubilities of both homo- and heterotrimers.

Figure 5c shows the solubility of the hetero- and homotrimers in equilibrium with fibrils containing different homotrimer fractions. As in previous reports,[19] we found the solubility of the homotrimers to be 15–20 times higher than that of the heterotrimers in pure samples. The solubility of the homotrimers decreased with their decreasing

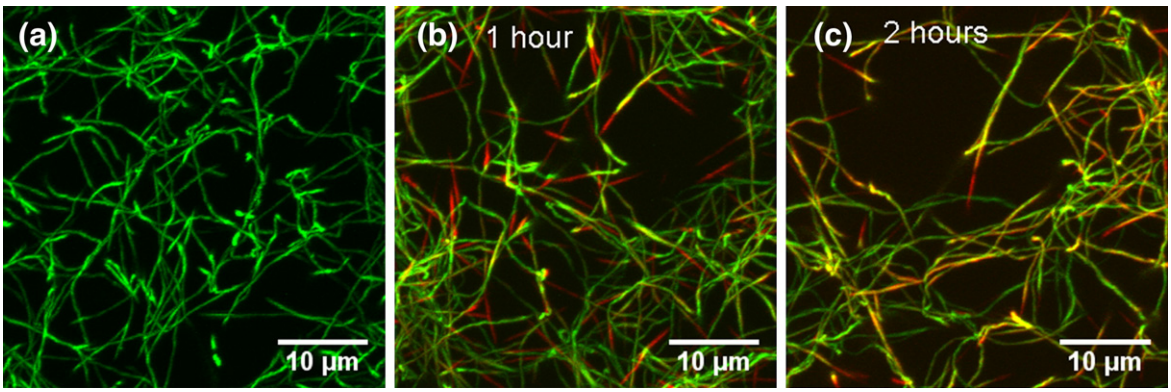

Fig. 4. 3D reconstruction of confocal images illustrating interaction of homotrimers with preassembled heterotrimer fibrils. (a) Heterotrimer-G fibrils before addition of homotrimer-R solution. (b) Mixed fibrils after 1-h (b) and 2-h (c) equilibration with added homotrimer solution at 32 °C.

Author's personal copy

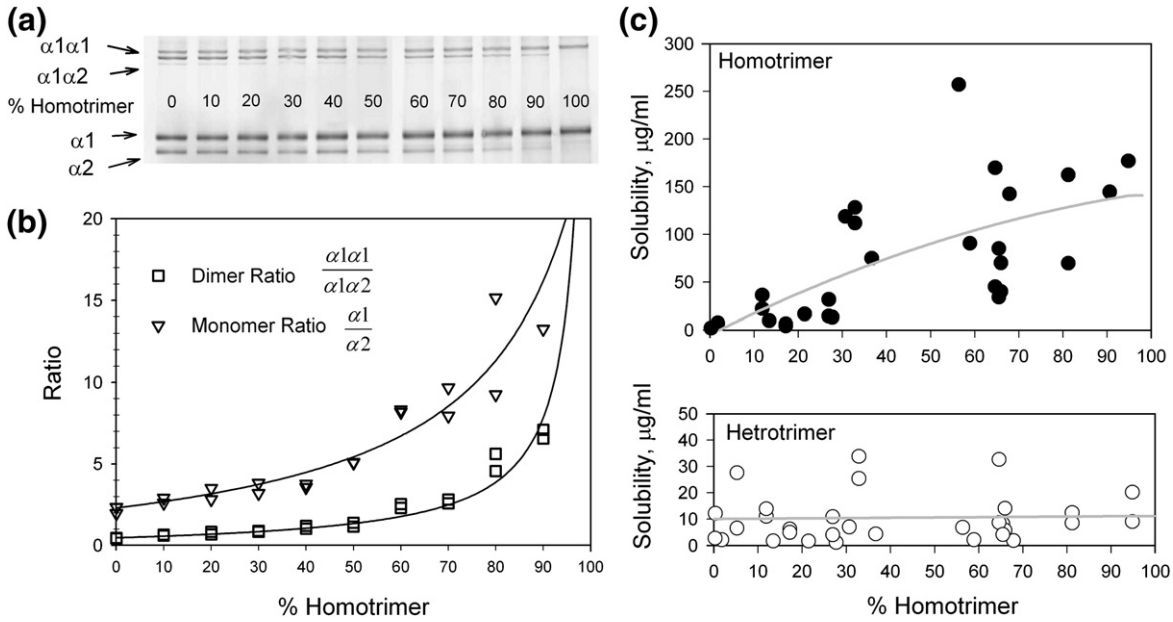

Fig. 5. Measurement of homo- and heterotrimer solubility by gel electrophoresis. (a) Monomer and dimer gel bands of type I collagen chains in different initial mixtures. (b) Calibration curves for monomer (α1/α2) and dimer (α1α1/α1α2) fluorescent intensity ratios of the corresponding bands shown on the gel. (c) Concentrations of soluble homo- and heterotrimer in equilibrium with fibrils after overnight equilibration at 32 °C plotted *versus* fibril composition. The soluble and fibrillar collagen fractions were separated by centrifugation and analyzed by gel electrophoresis.

fraction in fibrils, consistent with a simple ideal mixture model for the molecules within fibrils (Supplementary Material). In contrast, the solubility of the heterotrimers was independent of the overall fibril composition, inconsistent with the ideal mixture model. Such constant solubility, however, may be expected when a fraction of the heterotrimers is completely segregated from the homotrimers within some fibril regions (see Discussion).

Discussion

The spear shape of homotrimer fibrils indicates increased bending stiffness

We found that pepsin-treated homotrimers formed more rigid, spearlike fibrils compared to flexible, threadlike heterotrimer fibrils (Fig. 2). Previously, the spearlike morphology was reported for both homotrimers[19] and heterotrimers.[35] In our experiments, all fibrils were thinner than in these previous studies, making them more susceptible to bending by thermal fluctuations and weak convective flows, but only heterotrimer fibrils exhibited significant bending.

The apparent higher bending rigidity of homotrimer fibrils cannot be explained by their thickness, packing, or intermolecular cross-linking. Homotrimer fibrils have the same D-periodic axial alignment of molecules[20] and lower lateral density in the cross section.[18,20] In addition, our homotrimer fibrils were thinner than heterotrimer fibrils, which should make them easier rather than more difficult to bend. Formation of covalent cross-links, which might affect the bending rigidity, was precluded by the pepsin treatment.

Thus, the increased homotrimer fibril stiffness is likely to be related to the rigidity of their component triple helices. Since bending distorts helical structure, higher stability of homotrimer helices[16,17] may contribute to their increased rigidity. The reported difference in the pattern of flexible and rigid regions within homo- and heterotrimer helices[17] may also contribute by altering the alignment of these regions on adjacent molecules. The increased rigidity of homotrimer fibrils may play an important role, e.g., in the reduced tensile strength of tendons[21] and increased bone fragility[16] in oim mice.

Nonfibrillar aggregates nucleate fibrillogenesis of pepsin-treated homotrimers

Although homotrimers have higher solubility[19] and exhibit weaker intermolecular attraction in fibrils,[18] they assemble into fibrils without the lag phase,[17] i.e., fibril nucleation occurs much faster in homotrimers than in heterotrimers. Our new findings not only confirm the latter counterintuitive observation but also suggest why this observation may not conflict with less efficient recognition between homotrimers.

The appearance of homotrimer fibrils as multiple spears growing from a common center indicates that heating from 4 to 32 °C induces nonspecific, rapid aggregation of homotrimers into nonfibrillar clumps without proper mutual alignment of molecules. The fibrils are nucleated within these aggregates. They grow outward in several directions resulting in the characteristic morphology of multiple spears

Author's personal copy

emanating from a common center (Fig. 2). The interactions causing the initial, nonspecific aggregation may be weaker than the recognition and attraction at the proper alignment, but they seem to have no energy barrier. Thus, the aggregation proceeds rapidly, although the energy gain from it may be lower than from proper fibril assembly. It is detected by light scattering as the initial phase of fibrillogenesis, so that the solution turbidity increases without a lag phase. The kinetics of formation of homotrimer fibrils with properly aligned molecules is masked by this aggregation. Presently, we do not know whether it is slower or faster than the formation of heterotrimer fibrils.

Fibrillogenesis of pepsin-treated heterotrimers does not involve formation of nonfibrillar aggregates. Heterotrimers remain undetected by light scattering or confocal microscopy during the lag phase until they overcome a nucleation barrier and assemble into well-defined fibrils. Note that the heterotrimer nucleation barrier may be higher, although their mutual interactions in fibrils at equilibrium are more favorable than between homotrimers. The observed initial kinetics of heterotrimer fibril formation was slower than for homotrimers because it involves higher-energy intermediates. This does not contradict more favorable equilibrium interactions between heterotrimers within fibrils.

Interestingly, rapid formation of nonfibrillar aggregates after the temperature jump was also observed in homo- and heterotrimer mixtures (Fig. 1), but not when the homotrimers were added to preformed heterotrimer fibrils (Fig. 4). The latter observation suggests that homotrimer binding at tips of heterotrimer fibrils occurs without a significant energy barrier and that this binding is more energetically favorable than the nonfibrillar aggregation.

The nonfibrillar aggregation seems to be a property of only pepsin-treated α1(I) homotrimers with partially degraded telopeptides; i.e., it is prevented by the α2(I) chain and by α1(I) telopeptides. Indeed, pepsin-treated heterotrimers containing the α2(I) chain do not form such nonfibrillar aggregates. Full-length homotrimer molecules with intact α1(I) telopeptides, which were not treated by pepsin, were also reported to form isolated spears rather than hedgehog-like spear clusters after a normal lag phase.[19] By preventing the nonspecific aggregation, the α2(I) chain and the telopeptides may play an important role in initial reorientation and alignment of triple helices required for fibril formation.

Homo- and heterotrimers co-assemble within the same fibril but segregate at a subfibrillar level

The observed multistep kinetics of fibril formation (Fig. 1c) suggests the following sequence of events in mixtures of pepsin-treated homo- and heterotrimers. Based on the properties of pure homo- and heterotrimers, the first step of early growth likely involves fast nonfibrillar aggregation of homotrimers followed by the outward growth of homotrimer fibrils. The next step (lag phase) involves nucleation of mixed homo/heterotrimer fibrils or predominantly heterotrimer fibrils, which may be promoted by binding of heterotrimers to the homotrimer aggregates and fibrils. Provided that the binding/diffusion time is shorter than the nucleation time, such binding may explain why the lag time at this step appears to be independent of the heterotrimer fraction in the mixture. The growth of heterotrimer-enriched fibril regions from these nuclei occurs at the delayed growth step of the turbidity curve.

The sequential formation of homo- and heterotrimer-enriched fibril regions may contribute to the subfibrillar segregation observed in our experiments. The appearance of homotrimers at fibril tips may be related, e.g., to their higher solubility and, therefore, lower binding energy. Once formation of heterotrimer-enriched fibrils is nucleated, it proceeds faster than homotrimer binding or assembly, depleting the surrounding solution of heterotrimers. The remaining homotrimers bind last, thereby appearing at fibril tips. It is also possible, however, that homotrimers preferentially bind at fibril tips due to the different geometry of intermolecular contacts at the growing tip *versus* the side surface.

In addition to kinetics, subfibrillar segregation of homo- and heterotrimers may result from equilibrium interactions, as indicated by the persistence of the segregation after overnight or longer equilibration. Pepsin-treated collagen molecules dissociate from and reassociate with fibrils, since they do not form intermolecular cross-links. The equilibrium between fibril surfaces and surrounding solution was previously found to be established after several hours.[36] Consistently, here we observed significant fibril remodeling several hours after addition of homotrimers to preformed heterotrimer fibrils. After initial association at tips of heterotrimer fibrils, the homotrimers gradually appeared along the whole length of the fibrils and the heterotrimers appeared in the places where the fibril tips were elongated (Fig. 4). We should note, however, that complete reequilibration of composition in fibril cores may take much longer than at fibril surfaces and may not be practically attainable.

Additional evidence for equilibrium segregation of homo- and heterotrimers is the dependence of their equilibrium solubility on the mixture composition (Fig. 5). At equilibrium between a homogeneously mixed binary aggregate and a surrounding solution, the solubility of the minor component should be approximately proportional to its fraction within the aggregate provided that this fraction is sufficiently small (Supplementary Material). We observed such proportionality from 0% up to ~30% of homotrimers in aggregates, suggesting that a relatively small amount of homotrimers can be well mixed with heterotrimers. In contrast, the solubility of heterotrimers did not change when

Author's personal copy

their fraction was varied, suggesting poor mixing of the molecules in fibrils containing a small fraction of heterotrimers.

Much lower solubility of the heterotrimers[19] (Fig. 5) and their segregation suggest that heterotrimer–heterotrimer interactions in fibrils are much more energetically favorable than homotrimer–homotrimer and heterotrimer–homotrimer interactions. Presently, we do not know which of the latter two interactions is more favorable than the other. The asymmetric segregation, which occurs at a low fraction of heterotrimers but not at a low fraction of homotrimers, significantly complicates evaluation of the heterotrimer–homotrimer interaction energy. It indicates, e.g., that the heterotrimer–homotrimer interaction may be different for a homotrimer surrounded by heterotrimers and for a heterotrimer surrounded by homotrimers.

Biomedical implications

The subfibrillar segregation may significantly enhance the effect of even a small homotrimer fraction on the collagen fibril integrity and mechanical properties because the homotrimers have different triple helix stability, stretching elasticity, and bending rigidity. The segregation certainly occurs *in vitro* in fibrils assembled from pepsin-treated collagen molecules with partially degraded telopeptides. *In vivo*, the fibrils assemble from molecules with intact telopeptides in a different environment and under different conditions. Not only is it a nonequilibrium process, but it also may be actively regulated by cells.[37] The resulting fibrils are stabilized by irreversible covalent cross-links. Their remodeling involves proteolytic degradation of old collagen and its replacement with newly synthesized molecules rather than equilibrium dissociation and reassociation of the molecules. Unfortunately, differential fluorescent labeling and direct observation of the subfibrillar segregation *in vivo* or even in cell culture is presently unrealistic.

Still, our findings suggest that the tendency of homo- and heterotrimers to segregate, particularly the kinetic segregation, is likely to be preserved *in vivo* as well. The dramatic difference between pepsin-treated homotrimers and pepsin-treated heterotrimers indicates that the α2(I) chain plays a major role in both kinetic and equilibrium segregation, although telopeptides may inhibit the formation of nonfibrillar aggregates *in vivo*. Involvement of tissue collagenases in fibril remodeling may further exaggerate the segregation because α1(I) homotrimers are less susceptible than the heterotrimers to cleavage by these enzymes.[38]

If this hypothesis is correct, even a small fraction of α1(I) homotrimers may have a large effect on tissues. For instance, accumulation of homotrimers with multiple bone remodeling cycles may exacerbate gradual degradation of bone quality with age in individuals with the overproducing allele of *COL1A1*, increasing osteoporotic fractures. Synthesis and accumulation of collagenase-resistant homotrimers inside kidney glomeruli may result in glomerular sclerosis contributing to renal failure.[39] Similarly, accumulation of collagenase-resistant homotrimer-rich fibrils or subfibrillar regions may play a detrimental role in a broader spectrum of fibrotic tissues and disorders.

Materials and Methods

Native collagen

Pepsin-soluble collagen was purified from tail tendons of wild-type (normal heterotrimers) and homozygous *oim* mice [α1(I) homotrimers] as previously described.[18] Briefly, frozen mouse tails were thawed in ice-cold 3.5 M NaCl, 10 mM Tris, 20 mM ethylenediaminetetraacetic acid, 2 mM *N*-ethylmaleimide, and 1 mM phenylmethylsulfonyl fluoride (pH 7.5). Tendons were excised from tails, washed in the same enzyme-inhibiting buffer for several days at 4 °C, dissolved in 0.5 M acetic acid (pH 2.8), and digested by pepsin (100 mg/1 g collagen in two doses each for 24 h at 4 °C). After removal of insoluble material by centrifugation, collagen was precipitated overnight by 0.9 M NaCl, separated by centrifugation, redissolved in 0.5 M acetic acid, and reprecipitated by 0.7 M NaCl. The final precipitate was resuspended and extensively dialyzed against excess 2 mM HCl. The resulting collagen was characterized by gel electrophoresis using the same procedure as described in the *In vitro* fibrillogenesis section. The concentration of collagen was evaluated by circular dichroism (CD) on a J810 spectrometer (Jasco Inc.).

Reconstituted α1(I) homotrimers

Type I collagen from rat tails and fetal calf tendons (both from Pel-Freez Biologicals) was prepared by the same method. The pepsin-soluble collagen was transferred into 0.2 M sodium phosphate, 0.5 M glycerol (pH 7.4), diluted to 0.8 mg/ml, denatured at 55 °C for 10 min, and refolded at 26 °C for 10 days. The CD spectra of solution aliquots at room temperature were measured to control the extent of denaturation and refolding. The refolded collagen was dialyzed into 0.5 M acetic acid at 4 °C, digested by pepsin (0.2–0.9 mg/ml) for 40 min at 32 °C followed by 2–3 h at room temperature (to remove partially folded molecules and residual heterotrimers), and precipitated by 1 M NaCl overnight at 4 °C. The precipitate was resuspended in and dialyzed against 2 mM HCl, mixed 1:1 (v/v) with 0.26 M NaCl, 60 mM sodium phosphate, pH 7.4 (after mixing), and reprecipitated by overnight fibrillogenesis at 32 °C (to remove residual impurities and fibrillogenesis-incapable molecules). Fibrillar collagen was separated by centrifugation, resuspended in and dialyzed against 2 mM HCl, and characterized by gel electrophoresis, CD, and differential scanning calorimetry at 1 °C/min in N-DSC II (Calorimetry Sciences Corp.).[40]

In vitro fibrillogenesis

For kinetic measurements, a pepsin-treated collagen solution in 2 mM HCl was mixed 1:1 with 40 or 60 mM sodium phosphate, 0.26 M NaCl (pH 7.4 after mixing) at 4 °C. The solution was degassed, transferred into a quartz cuvette (1-cm optical path) precooled at 4 °C and placed

Author's personal copy

into a V-560 spectrophotometer (Jasco Inc.) equipped with a thermoelectric temperature controller set at 4 °C. Fibrillogenesis was initiated by a temperature jump to 32 °C. Once the temperature reached 32 °C, the time evolution of the solution turbidity was monitored by measuring the optical density at 350 nm.

For solubility measurements, different mixtures of mouse homo- and heterotrimer in 2 mM HCl were mixed 1:1 with 60 mM sodium phosphate, 0.26 M NaCl, 0.03% Brij 35 (pH 7.4 after mixing) and equilibrated for 1 day at 32 °C. The fibrils and surrounding solutions were separated by 30-min centrifugation at 20,000*g*. The supernatants were collected with pipette tips rinsed with 0.03% Brij 35 into tubes also rinsed with 0.03% Brij 35. Pellets resuspended in 2 mM HCl and supernatants were mixed 4:1 with 2.5 M NaCl, 0.5 M sodium carbonate, pH 9.3. Each sample was then rapidly mixed 5:1 with freshly prepared monoreactive Cy5 NHS ester (GE Healthcare PA 35001) solution in anhydrous dimethylformamide (1 vial/ml) and immediately placed on a shaker for 30 min at room temperature. The same stock solution of the dye was used for all labeling reactions to ensure the same labeling efficiency. The accuracy of the labeling was tested by adding bovine serum albumin to some of the samples as an internal standard.[36] After 30-min labeling, the samples were mixed with 4× NuPAGE LDS Sample Buffer (Invitrogen), denatured at 60 °C for 5 min, and separated on precast 3–8% Tris–acetate minigels (Invitrogen). The gels were scanned on a FLA5000 fluorescence scanner (Fuji Medical Systems) and analyzed by Multi Gauge 3.0 software supplied with the scanner.

Confocal imaging

Collagen solution in 2 mM HCl was mixed 4:1 with 2.5 M NaCl and 0.5 M sodium carbonate (pH 9.3) and fluorescently labeled with 2–10 μg/ml Alexa Fluor 488 or Alexa Fluor 568 carboxylic acid succinimidyl ester (Invitrogen). The amount of the dye was adjusted to result in one attached dye molecule per four to five collagen triple helices. After 30-min labeling at room temperature, the reaction was stopped and collagen was precipitated by adding acetic acid to 0.5 M and NaCl to 0.9 M. After overnight equilibration, precipitated collagen was separated by centrifugation, resuspended in 2 mM HCl and extensively dialyzed against 2 mM HCl to remove residual free dye molecules. To evaluate the labeling efficiency, the collagen concentration was determined by CD at 221 nm. The concentration of the conjugated dye was determined from visible light absorption in a Lambda 900 spectrometer (Perkin Elmer) as recommended by the dye manufacturer.

Binary mixtures of collagens labeled by Alexa Fluor 488 and Alexa Fluor 568 were mixed 1:1 with 60 mM sodium phosphate, 0.26 M NaCl (pH 7.4 after mixing), transferred into SecureSeal hybridization chambers (Grace Bio-Labs), and sealed. The cover glass used with the chambers was pretreated by Sigmacote (Sigma) to prevent attachment of collagen fibrils. The hybridization chambers were attached to microscope slides and preequilibrated at 32 °C or directly mounted on a microscope stage in a controlled environment chamber set at 32 °C. The fibrils were imaged in a Zeiss 510 Inverted Meta confocal laser-scanning microscope (Carl Zeiss) with a 488-nm argon ion laser and a 543-nm helium–neon laser. The emission was collected by independent photomultipliers in two channels with 505- to 530-nm band-pass and 560-nm long-pass filters. The sample was illuminated by only one of the lasers at any given time, utilizing a line scanning mode with automatic laser switching. Virtually no Alexa Fluor 568 signal was detected in the Alexa Flour 488 channel and *vice versa*. The digital zoom, *z*-oversampling, scanning rate, and laser power were optimized to eliminate photobleaching.

Image processing and color separation analysis

A nonuniform background caused by interference and reflections was subtracted with Image J software†. The residual noise was eliminated with an intensity threshold that did not affect colors within fibrils. Three-dimensional images were reconstructed with MIPAV software‡. For color separation analysis, both channels were normalized to the same total intensity within each 3D stack. The color separation ratio

$$\frac{I_R - I_G}{I_R + I_G}$$

was calculated for each pixel, where I_R and I_G were normalized intensities of the red and green channels, respectively. The color separation within fibrils was characterized by histograms of the relative frequency of $(I_R - I_G)/(I_R + I_G)$ from −1.0 to 1.0 with 0.1 step.

Acknowledgements

We are grateful to Natalia Kuznetsova and Elena Makareeva for valuable discussions and suggestions. Confocal microscopy was performed at the Microscopy and Imaging Core of the National Institute of Child Health and Human Development (NICHD) with the assistance of Dr. Vincent Schram. This work was supported in part by the Intramural Research Program of NICHD, National Institutes of Health (NIH), Department of Health and Human Services. Wolfgang Losert was partially supported by NIH grant R21-EB-00328501. Daniel McBride was supported by the Charitable and Research Foundation and the Arthritis Foundation.

Supplementary Data

Supplementary data associated with this article can be found, in the online version, at doi:10.1016/j.jmb.2008.08.008

References

1. Prockop, D. J. & Kivirikko, K. I. (1995). Collagens: molecular biology, diseases, and potentials for therapy. *Annu. Rev. Biochem.* **64**, 403–434.
2. Brodsky, B. & Eikenberry, E. F. (1982). Characterization of fibrous forms of collagen. *Methods Enzymol.* **82 Pt. A**, 127–174.

† http://rsb.info.nih.gov/ij/
‡ http://mipav.cit.nih.gov/

Author's personal copy

3. Kelly, J., Tanaka, S., Hardt, T., Eikenberry, E. F. & Brodsky, B. (1988). Fibril-forming collagens in lamprey. *J. Biol. Chem.* **263**, 980–987.
4. Jimenez, S. A., Bashey, R. I., Benditt, M. & Yankowski, R. (1977). Identification of collagen alpha1(I) trimer in embryonic chick tendons and calvaria. *Biochem. Biophys. Res. Commun.* **78**, 1354–1361.
5. Moro, L. & Smith, B. D. (1977). Identification of collagen alpha1(I) trimer and normal type I collagen in a polyoma virus-induced mouse tumor. *Arch. Biochem. Biophys.* **182**, 33–41.
6. Rojkind, M., Giambrone, M. A. & Biempica, L. (1979). Collagen types in normal and cirrhotic liver. *Gastroenterology*, **76**, 710–719.
7. Haralson, M. A., Jacobson, H. R. & Hoover, R. L. (1987). Collagen polymorphism in cultured rat kidney mesangial cells. *Lab. Invest.* **57**, 513–523.
8. Rupard, J. H., Dimari, S. J., Damjanov, I. & Haralson, M. A. (1988). Synthesis of type I homotrimer collagen molecules by cultured human lung adenocarcinoma cells. *Am. J. Pathol.* **133**, 316–326.
9. Ghersi, G., La Fiura, A. M. & Minafra, S. (1989). Direct adhesion to type I and homotrimer collagens by breast carcinoma and embryonic epithelial cells in culture: a comparative study. *Eur. J. Cell Biol.* **50**, 279–284.
10. Gibbs, S. R., Goins, R. A., Belvin, E. L., Dimari, S. J., Merriam, A. P., Bowling-Brown, S. *et al.* (1999). Characterization of the collagen phenotype of rabbit proximal tubule cells in culture. *Connect Tissue Res.* **40**, 173–188.
11. Nicholls, A. C., Osse, G., Schloon, H. G., Lenard, H. G., Deak, S., Myers, J. C. *et al.* (1984). The clinical features of homozygous alpha 2(I) collagen deficient osteogenesis imperfecta. *J. Med. Genet.* **21**, 257–262.
12. Sasaki, T., Arai, K., Ono, M., Yamaguchi, T., Furuta, S. & Nagai, Y. (1987). Ehlers–Danlos syndrome. A variant characterized by the deficiency of pro alpha 2 chain of type I procollagen. *Arch. Dermatol.* **123**, 76–79.
13. Hata, R., Kurata, S. & Shinkai, H. (1988). Existence of malfunctioning pro alpha2(I) collagen genes in a patient with a pro alpha 2(I)-chain-defective variant of Ehlers–Danlos syndrome. *Eur. J. Biochem.* **174**, 231–237.
14. Schwarze, U., Hata, R., McKusick, V. A., Shinkai, H., Hoyme, H. E., Pyeritz, R. E. & Byers, P. H. (2004). Rare autosomal recessive cardiac valvular form of Ehlers–Danlos syndrome results from mutations in the COL1A2 gene that activate the nonsense-mediated RNA decay pathway. *Am. J. Hum. Genet.* **74**, 917–930.
15. Pace, J. M., Wiese, M., Drenguis, A. S., Kuznetsova, N., Leikin, S., Schwarze, U. *et al.* (2008). Defective C-propeptides of the Pro{alpha}2(I) chain of type I procollagen impede molecular assembly and result in osteogenesis imperfecta. *J. Biol. Chem.* **283**, 16061–16067.
16. Miles, C. A., Sims, T. J., Camacho, N. P. & Bailey, A. J. (2002). The role of the alpha2 chain in the stabilization of the collagen type I heterotrimer: a study of the type I homotrimer in oim mouse tissues. *J. Mol. Biol.* **321**, 797–805.
17. Kuznetsova, N. V., McBride, D. J. & Leikin, S. (2003). Changes in thermal stability and microunfolding pattern of collagen helix resulting from the loss of alpha2(I) chain in osteogenesis imperfecta murine. *J. Mol. Biol.* **331**, 191–200.
18. Kuznetsova, N., McBride, D. J., Jr. & Leikin, S. (2001). Osteogenesis imperfecta murine: interaction between type I collagen homotrimers. *J. Mol. Biol.* **309**, 807–815.
19. McBride, D. J., Jr., Kadler, K. E., Hojima, Y. & Prockop, D. J. (1992). Self-assembly into fibrils of a homotrimer of type I collagen. *Matrix*, **12**, 256–263.
20. McBride, D. J., Jr., Choe, V., Shapiro, J. R. & Brodsky, B. (1997). Altered collagen structure in mouse tail tendon lacking the alpha 2(I) chain. *J. Mol. Biol.* **270**, 275–284.
21. Misof, K., Landis, W. J., Klaushofer, K. & Fratzl, P. (1997). Collagen from the osteogenesis imperfecta mouse model (oim) shows reduced resistance against tensile stress. *J. Clin. Invest.* **100**, 40–45.
22. Minafra, S., Luparello, C., Rallo, F. & Pucci-Minafra, I. (1988). Collagen biosynthesis by a breast carcinoma cell strain and biopsy fragments of the primary tumour. *Cell Biol. Int. Rep.* **12**, 895–905.
23. Minafra, S., Minafra, I. P., Tomasino, R. M. & Sciarrino, S. (1984). Collagen composition in the ductal infiltrating carcinoma of human breast. *Cell Biol. Int. Rep.* **8**, 79–85.
24. Yamagata, S. & Yamagata, T. (1984). FBJ virus-induced osteosarcoma contains type I, type I trimer, type III as well as type V collagens. *J. Biochem.* **96**, 17–26.
25. Mann, V., Hobson, E. E., Li, B., Stewart, T. L., Grant, S. F., Robins, S. P. *et al.* (2001). A COL1A1 Sp1 binding site polymorphism predisposes to osteoporotic fracture by affecting bone density and quality. *J. Clin. Invest.* **107**, 899–907.
26. Grant, S. F., Reid, D. M., Blake, G., Herd, R., Fogelman, I. & Ralston, S. H. (1996). Reduced bone density and osteoporosis associated with a polymorphic Sp1 binding site in the collagen type I alpha 1 gene. *Nat. Genet.* **14**, 203–205.
27. Mann, V. & Ralston, S. H. (2003). Meta-analysis of COL1A1 Sp1 polymorphism in relation to bone mineral density and osteoporotic fracture. *Bone*, **32**, 711–717.
28. Ralston, S. H., Uitterlinden, A. G., Brandi, M. L., Balcells, S., Langdahl, B. L. & Lips, P. (2006). Large-scale evidence for the effect of the COLIA1 Sp1 polymorphism on osteoporosis outcomes: the GENOMOS study. *PLoS Med.* **3**, e90.
29. Chipman, S. D., Sweet, H. O., McBride, D. J., Jr., Davisson, M. T., Marks, S. C., Jr. & Shuldiner, A. R. (1993). Defective pro alpha 2(I) collagen synthesis in a recessive mutation in mice: a model of human osteogenesis imperfecta. *Proc. Natl Acad. Sci. USA*, **90**, 1701–1705.
30. Gelman, R. A., Poppke, D. C. & Piez, K. A. (1979). Collagen fibril formation *in vitro*. The role of the nonhelical terminal regions. *J. Biol. Chem.* **254**, 11741–11745.
31. Helseth, D. L., Jr. & Veis, A. (1981). Collagen self-assembly *in vitro*. Differentiating specific telopeptide-dependent interactions using selective enzyme modification and the addition of free amino telopeptide. *J. Biol. Chem.* **256**, 7118–7128.
32. Comper, W. D. & Veis, A. (1977). The mechanism of nucleation for *in vitro* collagen fibril formation. *Biopolymers*, **16**, 2113–2131.
33. Kuznetsova, N. & Leikin, S. (1999). Does the triple helical domain of type I collagen encode molecular recognition and fiber assembly while telopeptides serve as catalytic domains? Effect of proteolytic cleavage on fibrillogenesis and on collagen–collagen interaction in fibers. *J. Biol. Chem.* **274**, 36083–36088.
34. Veis, A. & Payne, K. (1988). Collagen fibrillogenesis. In *Collagen* (Nimni, M. E., ed.), Vol. I, pp. 113–137. CRC Press, Boca Raton, FL.
35. Kadler, K. E., Hulmes, D. J., Hojima, Y. & Prockop, D. J. (1990). Assembly of type I collagen fibrils de novo by the specific enzymic cleavage of pC collagen. The

Author's personal copy

fibrils formed at about 37 degrees C are similar in diameter, roundness, and apparent flexibility to the collagen fibrils seen in connective tissue. *Ann. N. Y. Acad. Sci.* **580**, 214–224.
36. Mertz, E. L. & Leikin, S. (2004). Interactions of inorganic phosphate and sulfate anions with collagen. *Biochemistry*, **43**, 14901–14912.
37. Canty, E. G. & Kadler, K. E. (2005). Procollagen trafficking, processing and fibrillogenesis. *J. Cell Sci.* **118**, 1341–1353.
38. Narayanan, A. S., Meyers, D. F., Page, R. C. & Welgus, H. G. (1984). Action of mammalian collagenases on type I trimer collagen. *Collagen Relat. Res.* **4**, 289–296.
39. Phillips, C. L., Pfeiffer, B. J., Luger, A. M. & Franklin, C. L. (2002). Novel collagen glomerulopathy in a homotrimeric type I collagen mouse (oim). *Kidney Int.* **62**, 383–391.
40. Leikina, E., Mertts, M. V., Kuznetsova, N. & Leikin, S. (2002). Type I collagen is thermally unstable at body temperature. *Proc. Natl Acad. Sci. USA*, **99**, 1314–1318.